Fluorescence of Covalently Attached Pyrene as a General RNA Folding Probe

Mary K. Smalley and Scott K. Silverman*

Department of Chemistry, University of Illinois at Urbana-Champaign, 600 South Mathews Avenue, Urbana, Illinois 61801

Table of Contents

Optimizing conditions for pyrene derivatization of RNA oligonucleotides

For RNA oligonucleotides with either a 2′-amino group (2′-NH_2) or a 2′-(2-aminoethoxy) group (2′-$OCH_2CH_2NH_2$; "tethered amine"), conditions for derivatization with the various pyrene STP esters were optimized on the analytical scale with 5′-^{32}P-radiolabeled RNA (Figure X1). A summary of the optimal derivatization conditions for all STP esters is provided in Table X1. In general, the derivatization reactions proceeded well in 100 mM sodium phosphate buffer. A pH value of 8.0 and solvent of 50% aqueous DMF generally worked best, with two exceptions as noted in the table caption. The optimal reaction temperature varied between 25 °C and 60 °C depending on the STP ester. The longer-chain esters generally required a higher temperature, likely for solubility reasons.

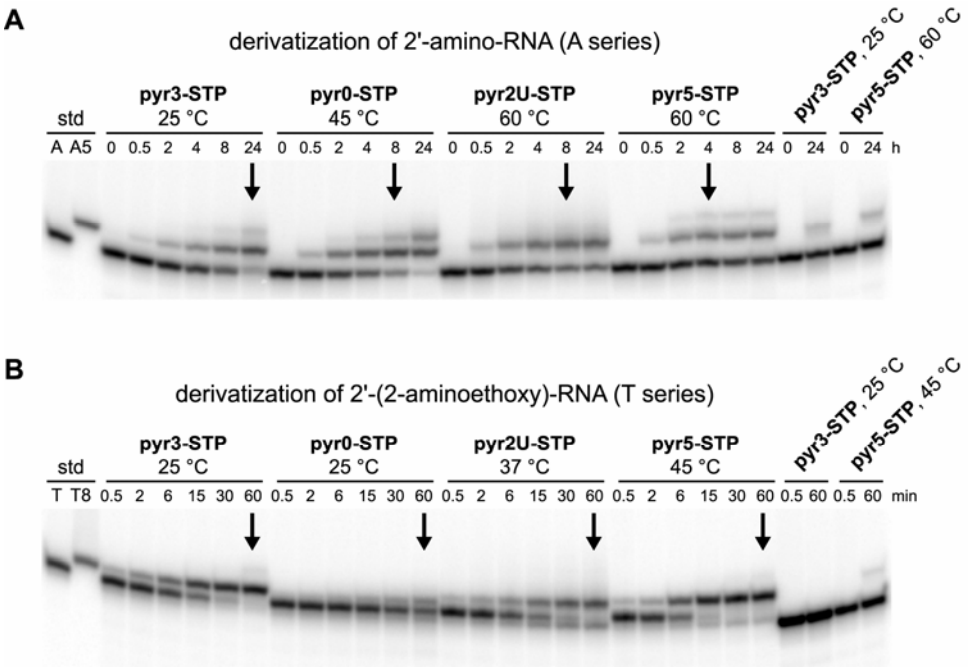

Figure X1. Representative experiments for optimizing pyrene derivatization conditions for (A) 2′-amino-RNA and (B) 2′-(2′-aminoethoxy)-RNA. In all cases, the assays were conducted in 20 µL total volume in 100 mM sodium phosphate (pH 8.0) with 10 µM RNA (trace 5′-^{32}P-radiolabeled; remainder cold-phosphorylated to avoid nonspecific loss of label) and 20 mM of the indicated pyrene-STP ester. Each assay was performed in 50% aqueous DMF except for reactions with **pyr0-STP**, which used 50% aqueous DMSO. The reaction temperature is given above each set of lanes. On the left two lanes of each gel, the standards are the unreacted amino RNA (A or T) and the corresponding A5- or T8-derivatized oligonucleotide. On the right four lanes of each gel, control reactions with the 2′-hydroxyl RNA are shown. These reactions illustrate the extent of nonspecific labeling under optimal **pyr3-STP** and **pyr5-STP** derivatization conditions (A-series, <12% in 24 h; T-series, <3% in 1 h). For all sets of lanes, the optimal timepoint used in practice for that particular STP ester is marked with an arrow. See Table X1 for the optimal derivatization conditions for all of the amine and STP ester combinations.

	incubation time, h	temperature, °C	yield, %	overderiv., % [a]
2′-amino-RNA				
pyr0-STP	8	45	60	10
pyr1-STP	8	45	40	<5
pyr2-STP	24	25	55	5
pyr2U-STP	8	60	50	<5
pyr3-STP	24	25	70	10
pyr4-STP	4	60	35 [b]	5
pyr5-STP	4	60	35 [b]	10
2′-(2-aminoethoxy)-RNA				
pyr0-STP	1	25	40	<5
pyr1-STP	1	25	75	<5
pyr2-STP	1	25	85	5
pyr2U-STP	1	37	65	<5
pyr3-STP	1	25	90	<5
pyr4-STP	1	37	90	<5
pyr5-STP	1	45	80	5

Table X1. Optimal derivatization conditions for 2′-amino-RNA and 2′-(2-aminoethoxy)-RNA, as determined from experiments such as those shown in Figure X1. All assays were conducted in 100 mM sodium phosphate buffer with 0.1 mM EDTA. The pH was 8.0 in all cases except for the **pyr1-STP** reactions, where pH 9.0 (bicine instead of sodium phosphate) was used on the basis of improved yield. The solvent was 50% aqueous DMF in all cases except for the **pyr0-STP** reactions, where 50% aqueous DMSO was used on the basis of improved yield. The pyrene-STP ester concentration was 20 mM in all cases.

[a] "Overderivatization" refers to the appearance of the higher-migrating secondary product visible in Figure X1. This secondary product presumably arises from further reaction of the primary pyrene-derivatized RNA. Overderivatization is quantified here as either <5%, 5%, or 10%.

[b] In these cases, yields were likely suppressed by limited solubility, because **pyr5-STP** and (to a lesser extent) **pyr4-STP** are not very soluble in 50% aqueous DMF.

Difference in basicity between 2′-amine (2′-NH_2) and 2′-tethered amine (2′-$OCH_2CH_2NH_2$)

The gel electrophoresis data indicate that the 2′-amino group and the 2′-(2-aminoethoxy) group have markedly different basicities (Figure X2). The latter is more basic, as revealed by the much slower migration of an RNA oligonucleotide incorporating the tethered amine relative to RNA with a 2′-hydroxyl or 2′-amino substituent at the same position. This increased basicity likely contributes to the greater nucleophilicity of the tethered amine relative to 2′-amino, as manifested in its much greater reactivity towards derivatization with pyrene STP esters (see Figure X1 above). Reduced steric concerns probably also contribute to the increased reactivity of the tethered amine.

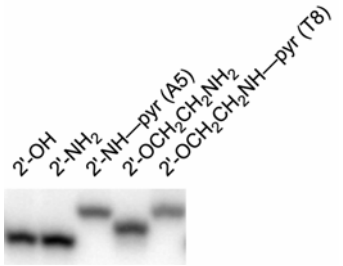

Figure X2. Denaturing PAGE of 15-mer RNA oligonucleotides corresponding to P4-P6 nucleotides 102-116 with various 2′-substituents at U107. Each RNA is 5′-^{32}P-radiolabeled; the gel running buffer is 1× TBE [89 mM each Tris and boric acid (pH 8.3)]. For each lane, the 2′-substituent at U107 is indicated. A5 and T8 correspond to pyrene-derivatized RNAs as described in the manuscript. Note the much slower migration of the 2′-tethered amino RNA (lane 4) compared with the 2′-hydroxyl and 2′-amino RNAs (lanes 1 and 2).

Quantitatively determining the basicity of the 2′-tethered amine from these types of experiments is challenging. We have not attempted gel electrophoresis experiments such as Figure X2 at different pH values, because such gels are best performed at specific pH values. However, we have performed pyrene derivatization experiments analogous to those of Figure X1 at pH 8.0, 7.0, and 6.0 (sodium phosphate buffer in each case). The reactivity of the 2′-tethered amine was lower at pH 7.0, and no reactivity at all was detected at pH 6.0 (data not shown). Therefore, we estimate that the pK_a value for the protonated 2′-tethered amine is between 6 and 8; we have not determined this value more precisely.

MALDI mass spectrometry data for pyrene-labeled RNAs

MALDI-MS data were obtained for several representative 24-mer pyrene-labeled oligoribonucleotides. The data are in Table X2.

oligonucleotide	calcd.	found	error
U247-T8	M^+ 7945.33	7948.54	+0.04%
U249-T8	M^+ 7945.33	7957.85	+0.16%
U253-T8	$[M+Na]^+$ 7968.32	7964.60	–0.05%
A246-T8	$[M+Na]^+$ 7968.32	7964.22	–0.05%

Table X2. MALDI-MS data for pyrene-labeled 24-nt RNA oligonucleotides.

MALDI-MS data were also obtained for several full-length (160-nt) pyrene-labeled P4-P6 RNAs. The data are in Table X3. Standards for the mass spectrometer were a 69-nt T7 RNA polymerase transcript with molecular weight 22216 and a T4 DNA ligase splint ligation product P4-P6-bp with molecular weight 51358.

P4-P6	calcd.	found	error
U107-A2	M^+ 51936.27	51968.32	+0.06%
U107-A5	M^+ 51978.35	52000.53	+0.04%
U107-T5	M^+ 51980.33	52009.21	+0.06%
U107-T8	M^+ 52022.41	52020.02	–0.01%
U107-T10	M^+ 52050.46	51991.00	–0.11%

Table X3. MALDI-MS data for pyrene-labeled 160-nt P4-P6 RNAs.

Fluorescence spectra for A2 derivatives at nucleotides other than U107

As shown in Figure 4A, an unusual feature was observed in the fluorescence emission spectrum of the U107-A2 derivative near 385 nm. Spectra from the equilibrium fluorescence titrations of the other P4-P6-A2 derivatives are shown in Figure X3. The unusual emission feature is observed at varying intensities in all of the spectra at high Mg^{2+} concentrations. The origin of this feature is unknown.

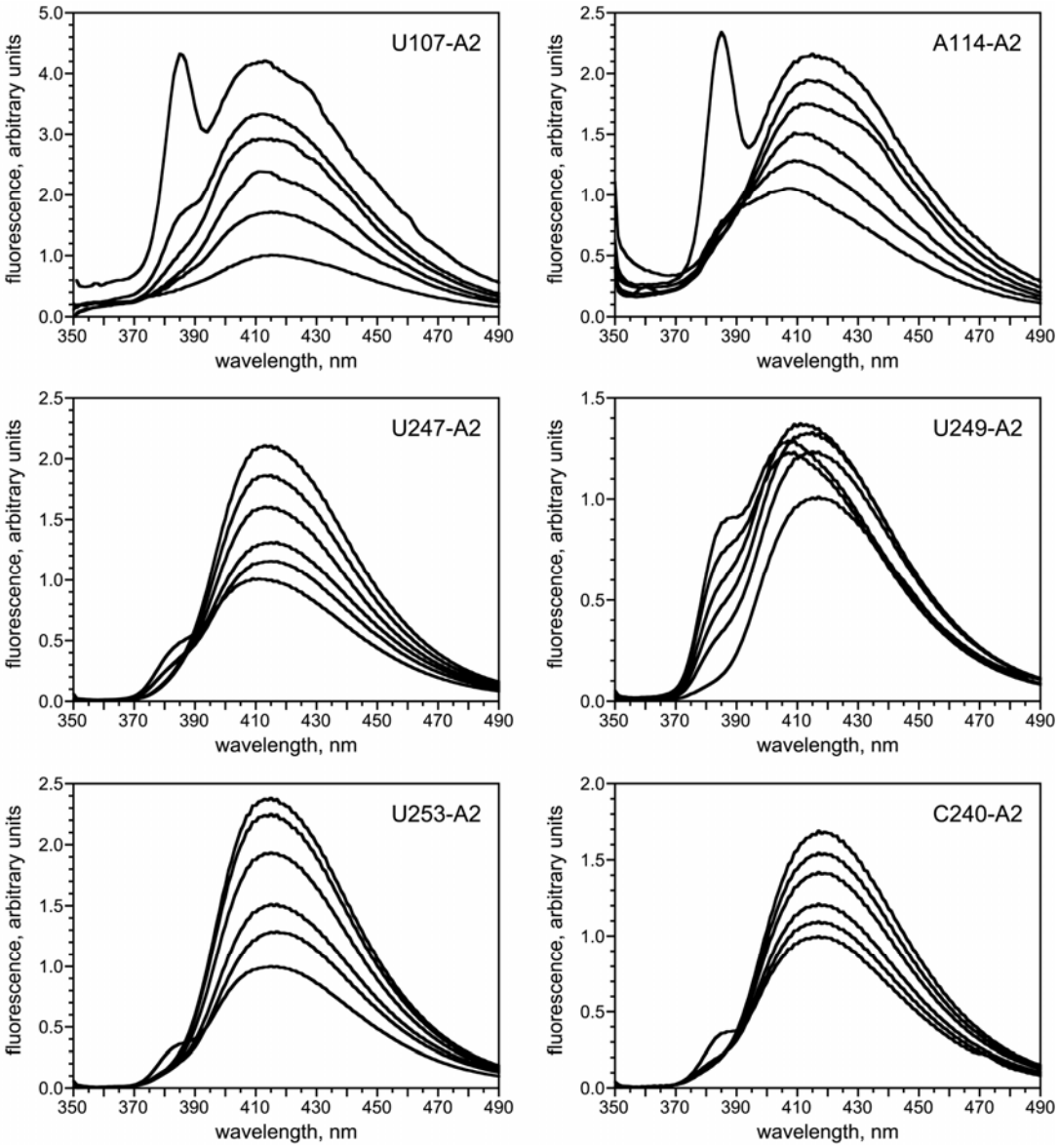

Figure X3. Fluorescence emission spectra showing representative data (1× TB buffer, 35 °C) for the indicated P4-P6 derivatives. The U107-A2 data from Figure 4A are shown for completeness. In all cases, the unusual emission peak near 385 nm is observed only at high Mg^{2+} concentrations (representative spectra shown from 0 to 400 mM Mg^{2+}). The size of the unusual 385-nm peak is strongly dependent on the nucleotide site of pyrene labeling. The relative emission intensities near 420 nm as a function of Mg^{2+} concentration are depicted in Figures 4 and 5. The A2 derivatives of A246 and A256 were not examined in this study.

Evidence for pyrene excimer formation with C240-T10 RNA derivatives

The C240-T10 24-mer RNA oligonucleotide was titrated with Mg^{2+} as in Figure 5. The concentration of 24-mer was either 100 or 400 nM, and the 136-nucleotide RNA that comprises the remainder of P4-P6 was either absent altogether (–) or present in four-fold excess (+). In all four cases, strong excimer emission was observed (Figure X4). The observation that the 24-mer alone shows excimer emission indicates that this phenomenon is not associated with P4-P6 tertiary folding. The observation that the relative strength of the excimer emission increases at higher RNA concentration for both the 24-mer alone and for P4-P6 is consistent with aggregation of either species as the source of excimer formation.

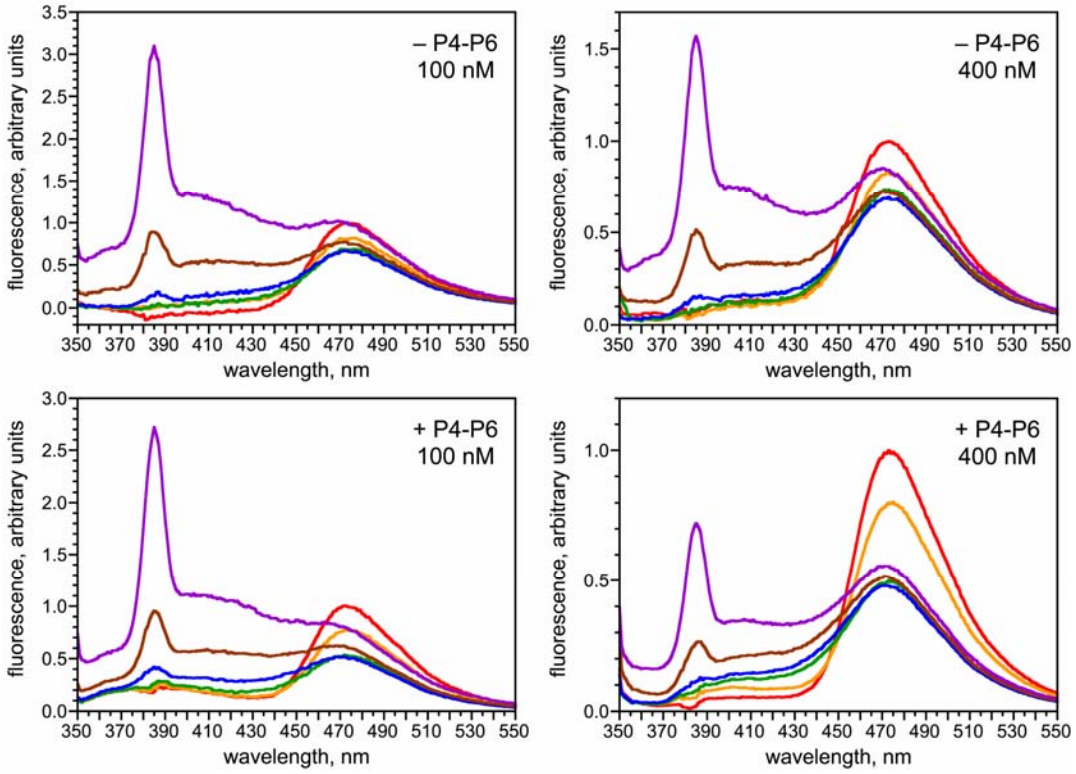

Figure X4. Fluorescence spectra for Mg^{2+} titrations of C240-T10 RNAs. Spectra are shown for Mg^{2+} concentrations of 0, 0.1, 1, 10, 100 and 300 mM (red, orange, green, blue, brown, and purple curves, respectively). All sets of spectra were normalized to fluorescence intensity = 1.0 at 473 nm for 0 mM Mg^{2+}. Note that the *x*-axis is extended to longer wavelength than for the fluorescence spectra shown in Figure 4 and Figure X3.

Experiments analogous to Figures 6 and 7 for the C240-T8 RNA

The experiments shown in Figures 6 and 7 provide strong evidence that pyrene fluorescence reports on P4-P6 tertiary folding for the tested derivatives. However, the C240-T8 derivative did not give similar data (Figure X5). In Figure X5A, the reconstituted P6 region has a fluorescence response essentially equivalent to that of the full C240-T8 P4-P6. On this basis, we cannot reasonably conclude that the tertiary folding of C240-T8 P4-P6 is reported by pyrene fluorescence. In Figure X5B, the C240-T8 P4-P6 was prepared either by ligation (Figure 3, path 1) or annealing (Figure 3, path 2), in both cases with either the wild-type GAAA tetraloop or the modified GAAAAA tetraloop that shifts the $[Mg^{2+}]_{1/2}$ value on native gels (see main text). In contrast to the four P4-P6 derivatives shown in Figure 7, the data here do not reveal a compelling shift in $[Mg^{2+}]_{1/2}$ due to the tetraloop modification. Again, on this basis we cannot reasonably conclude that tertiary folding of C240-T8 P4-P6 is reported by pyrene fluorescence.

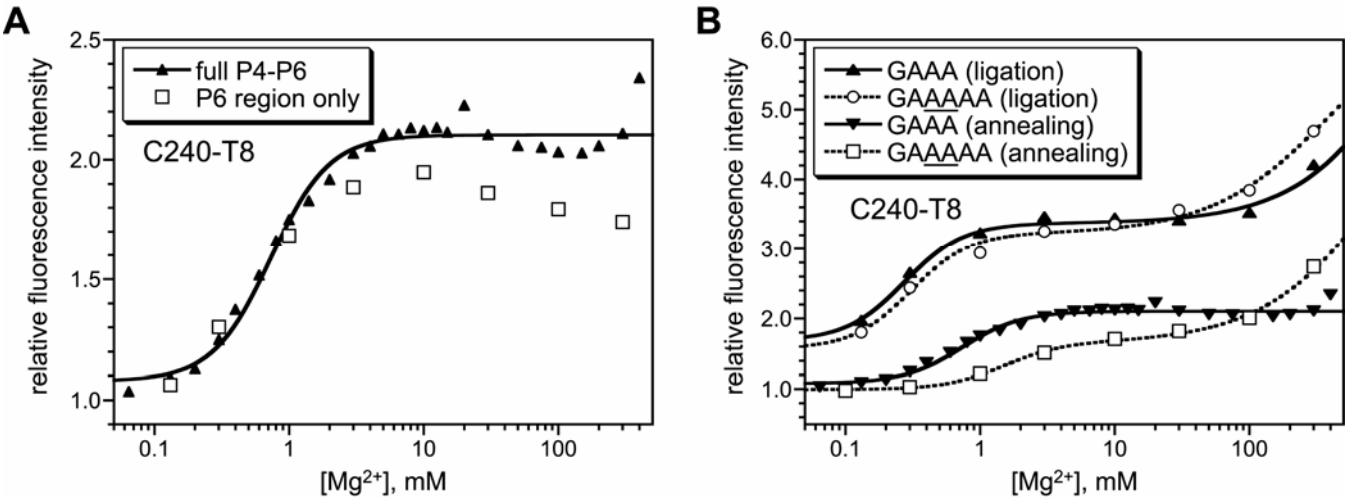

Figure X5. Experiments analogous to Figures 6 and 7 for the C240-T8 RNA. (A) Experiment analogous to Figure 6. (B) Experiments analogous to Figure 7, using P4-P6 RNA prepared as indicated either by ligation (Figure 3, path 1) or by annealing (Figure 3, path 2). The $[Mg^{2+}]_{1/2}$ values for the low-Mg^{2+} transitions were (top to bottom) 0.27 mM, 0.31 mM, 0.74 mM, and 1.50 mM.

Quantifying the fluorescence titration experiments

	$[Mg^{2+}]_{1/2}$, mM	I_0	I_1	I_2	I_A/I_0	I_B/I_A	Hill coefficients
U107							
A2	**0.65**	1.33	**3.01**	4.97	2.26	1.65	**2**,1
A3	**1.00**	1.36	**3.74**	7.83	2.75	2.09	**2**,1
A4	**0.89**	1.04	**2.59**	4.36	2.49	1.68	**2**,1
A5	**1.03**	0.99	**2.97**	4.96	3.00	1.67	**2**,1
A6	**0.88**	1.17	**3.54**	4.78	3.03	1.35	**2**,1
A7	**0.91**	1.17	**3.21**	5.78	2.74	1.78	**2**,1
T5	**0.65**	0.95	**6.95**	9.63	7.32	1.38	**2**,1
T6	**1.08**	1.25	**2.72**	3.98	2.18	1.46	**2**,1
T7	**1.01**	1.18	**4.05**	7.06	3.43	1.74	**2**,1
T8	**1.02**	1.19	**6.53**	8.91	5.49	1.36	**2**,1
T9	**0.84**	1.25	**4.20**	6.22	3.36	1.48	**2**,1
T10	**0.84**	1.13	**4.09**	6.02	3.62	1.47	**2**,1
A114							
A2	**0.64**	1.22	**1.78**	2.01	1.46	1.13	**2**,1
A5	**0.54**	1.08	**2.13**	4.15	1.97	0.51	**2**,1
T5	**1.23**	0.86	**2.30**	2.67	2.67	1.16	**2**,1
T8	**0.90**	1.05	**2.54**	3.36	2.42	1.32	**2**,1
T10	**0.89**	1.09	**5.31**	5.92	4.87	1.11	**2**,1
U247							
T5	**3.0**	1.54	**7.38**	9.14	4.79	1.24	**2**,1
T8	**3.5**	0.78	**3.28**	--	4.20	--	**2**
T10	**3.6**	0.70	**3.10**	3.84	4.43	1.24	**2**,1
U249							
A2	**4.0**	1.22	**4.95**	7.24	4.06	1.46	**2**,1
A5	**3.3**	0.95	**4.69**	6.25	4.94	1.33	**2**,1
T5	**3.2**	0.94	**2.52**	2.96	2.68	1.17	**2**,1
T8	**2.4**	0.95	0.55	**5.17**	5.44	--	1,**2**
T10	**2.9**	1.00	0.46	**8.23**	8.23	--	1,**2**
U253							
T8	**1.4**	0.58	**1.76**	[a]	3.03	[a]	**2**,1
T10	**0.9**	0.70	**3.07**	3.78	4.39	1.23	**2**,1
A246							
T5	**2.0**	1.06	**7.02**	6.03	6.62	0.86	**2**,1
T8	**2.5**	1.08	**15.83**	15.01	14.66	0.95	**2**,1
T10	**1.8**	1.06	**10.95**	10.47	10.33	0.96	**2**,1

Table X4. Curve fit parameters for the fluorescence titration data shown in Figures 4 and 5. I_0, I_1, and I_2 are the titration components for each fit (left to right on the Mg^{2+} axis). I_A is defined as the particular component assigned to tertiary folding (boldface entries), which in all but three cases is equivalent to I_1. I_B is the component after I_A along the Mg^{2+} axis. In all cases, the curve fit equation used the lowest Hill coefficients for each component that gave satisfactory curve fits. See ref. 16 for the curve fit equation and general approach. As detailed in ref. 16, the Hill coefficients could not be fit rather than being fixed; fitting the Hill coefficients led to poor curve fit convergence due to the large number of variables (>5). The $[Mg^{2+}]_{1/2}$ values are reproducible to <5% error between independent determinations.

[a] The I_B value could not be determined because the data at high $[Mg^{2+}]$ did not turn over (see Figure 5).

Native gel experiments

In Figure 8B are shown native gel Mg^{2+} titration data for individual pyrene-labeled P4-P6 RNAs. Such data were collected for additional key RNAs (Figure X6). As described in ref. 28, titration data were fit to the equation $M_{obs} = (M_{low} + M_{high} \bullet K \bullet [Mg^{2+}]^n)/(1 + K \bullet [Mg^{2+}]^n)$, where M_{obs} is the observed relative mobility as a function of $[Mg^{2+}]$; M_{low} and M_{high} are the limiting low and high values of relative mobility; and K and *n* are the equilibrium constant and Mg^{2+} Hill coefficient for the simple model equation $U + nMg^{2+} = F \bullet nMg^{2+}$ (U = unfolded state, F = folded state). The Mg^{2+} midpoint ($[Mg^{2+}]_{1/2}$ value) is $K^{-1/n}$. Values of $\Delta\Delta G°'$ were calculated as described in ref. 28, with $\Delta G°'$ for each RNA equal to $+nRT \bullet \ln [Mg^{2+}]_{1/2}$ ($\Delta\Delta G°'$ is defined as zero for wild-type P4-P6). A value of $n = 4$ was assumed in calculating all $\Delta\Delta G°'$ values, as previously described (ref. 28). Values of $[Mg^{2+}]_{1/2}$ and $\Delta\Delta G°'$ are collected in Table X5. A very good correlation between values $[Mg^{2+}]_{1/2}$ values from the independent native gel and fluorescence methods is documented in Figure 9.

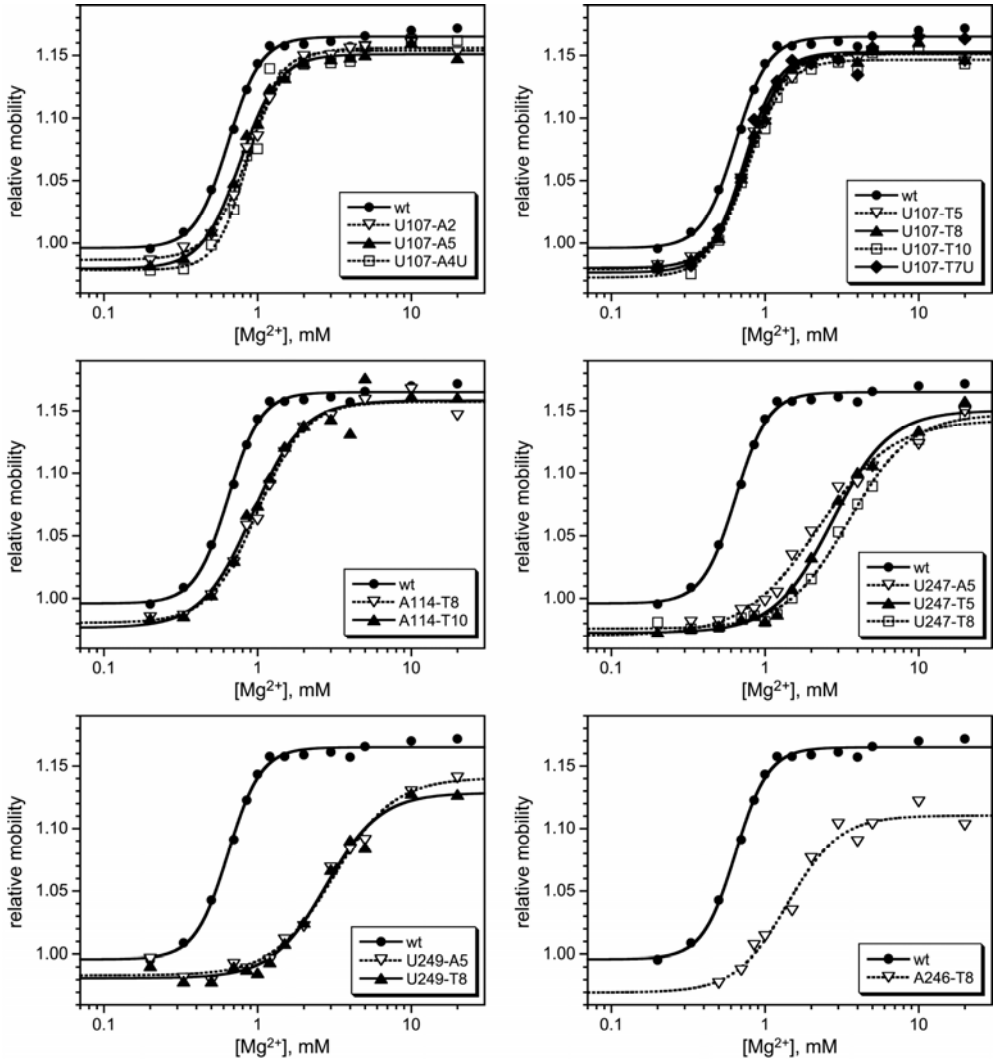

Figure X6. Native gel titration curves for pyrene-labeled P4-P6 RNAs (see text for equations).

P4-P6 RNA	$[Mg^{2+}]_{1/2}$, mM	n	ΔΔG°′, kcal/mol
wild-type	0.64	4.0	0
U107-A2	0.87	3.4	0.74
U107-A5	0.77	3.5	0.45
U107-T5	0.76	3.6	0.42
U107-T8	0.77	3.8	0.44
U107-T10	0.77	3.5	0.43
U107-A4U	0.86	4.3	0.72
U107-T7U	0.73	3.9	0.31
A114-T8	1.00	2.8	1.07
A114-T10	0.93	2.6	0.90
U247-A5	2.2	1.8	3.0
U247-T5	2.7	2.3	3.5
U247-T8	3.5	2.1	4.1
U249-A5	3.1	2.2	3.9
U249-T8	2.8	2.5	3.6
A246-T8	1.4	2.6	1.9

Table X5. Values computed from the native gel titration curves (see text for equations). The $[Mg^{2+}]_{1/2}$ values are reproducible to <5% error between independent determinations. This is equivalent to an error in ΔΔG°′ of <0.1 kcal/mol.

Accessibility of 2′-OH groups in the HDV ribozyme and 5S ribosomal subunit

To assess whether or not 2′-positions are generally reasonable candidate sites for pyrene modification, we examined the structures of two RNAs unrelated to P4-P6. For the HDV ribozyme (PDB id 1DRZ), there are 72 nucleotides in the X-ray crystal structure. The accessibility of each 2′-position was assessed by manual inspection of the structure using RasMol (Figure X7A). Each position was subjectively designated "accessible", "inaccessible", or "ambiguous" according to whether or not an appended substituent would appear to clash sterically with the remainder of the structure. Of the 72 nucleotides, 50 nt are accessible (69%); 14 nt are inaccessible (19%), and 8 nt are ambiguous (11%).

For the 5S RNA of the large ribosomal subunit (PDB id 1FFK), there are 122 nucleotides in the X-ray crystal structure. As for the HDV ribozyme, the accessibility of each 2′-position was assessed manually, both for the isolated 5S RNA alone (Figure X7B) and for the 5S RNA in the context of the remainder of the large ribosomal subunit (Figure X7C). For the 122 nt of the 5S RNA alone, 92 nt are accessible (75%), 14 nt are inaccessible (12%), and 16 nt are ambiguous (13%). For the 122 nt of the 5S RNA considered in the context of the remainder of the large ribosomal subunit, 82 nt are accessible (67%), 14 nt are inaccessible (12%), 14 nt are ambiguous (12%), and 12 nt contact the 23S RNA (10%).

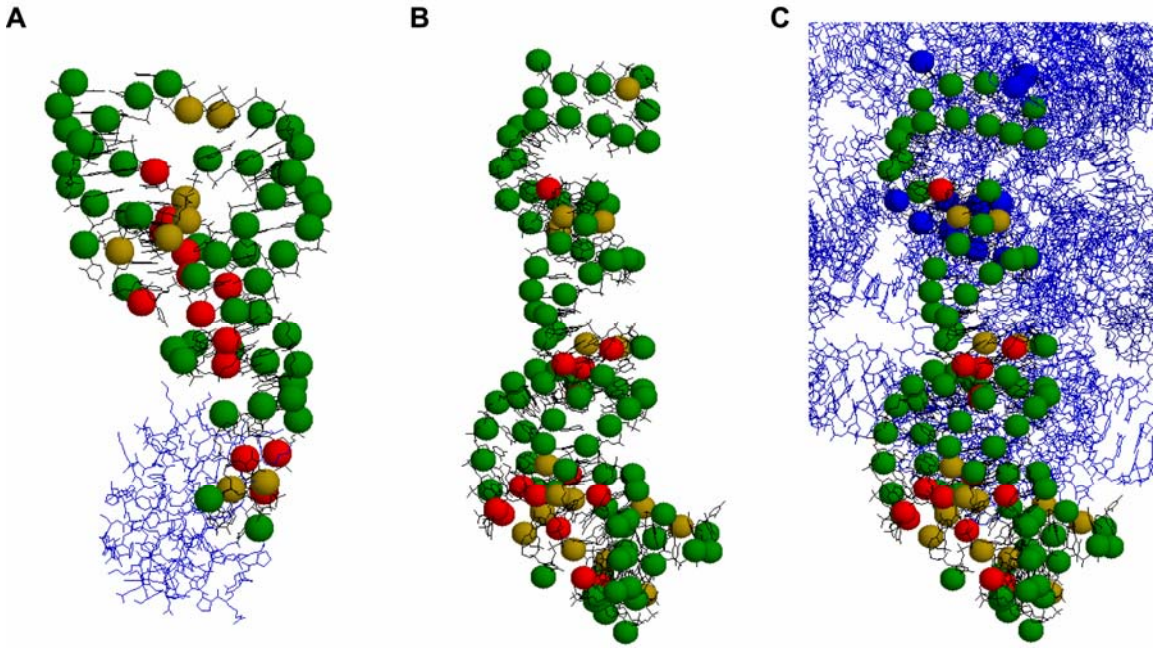

Figure X7. Accessibility of the 2′-positions of two structured RNAs. (A) The HDV ribozyme (PDB id 1DRZ). Color code for 2′-positions: green = accessible; red = inaccessible; yellow = ambiguous. Black wireframe denotes the RNA; blue wireframe is the co-crystallized U1A protein, which was ignored in assessing accessibility. (B) The 5S RNA in the large ribosomal subunit, without showing any of the other components of the ribosome (from PDB id 1FFK). Color code for 2′-positions: green = accessible; red = inaccessible; yellow = ambiguous. Black wireframe denotes the RNA. (C) The 5S RNA in the large ribosomal subunit, showing portions of domains II and V of the 23S RNA that are in contact with the 5S RNA. Color code for 2′-positions: green = accessible; red = inaccessible; yellow = ambiguous; blue = contacts 23S RNA. Black wireframe denotes the 5S RNA; blue wireframe is the 23S RNA.

Organic synthesis procedures and pyrene STP ester structures

The pyrene STP esters **pyr0-STP** through **pyr5-STP** (Figure X8A) were each prepared from the corresponding pyrene-substituted carboxylic acid **pyr0-COOH** through **pyr5-COOH** by DCC condensation as shown in Figure X8B. The carboxylic acids were obtained from commercial sources except for **pyr2-COOH**, **pyr2U-COOH**, and **pyr4-COOH**, which were prepared by straightforward procedures (Figure X8C).

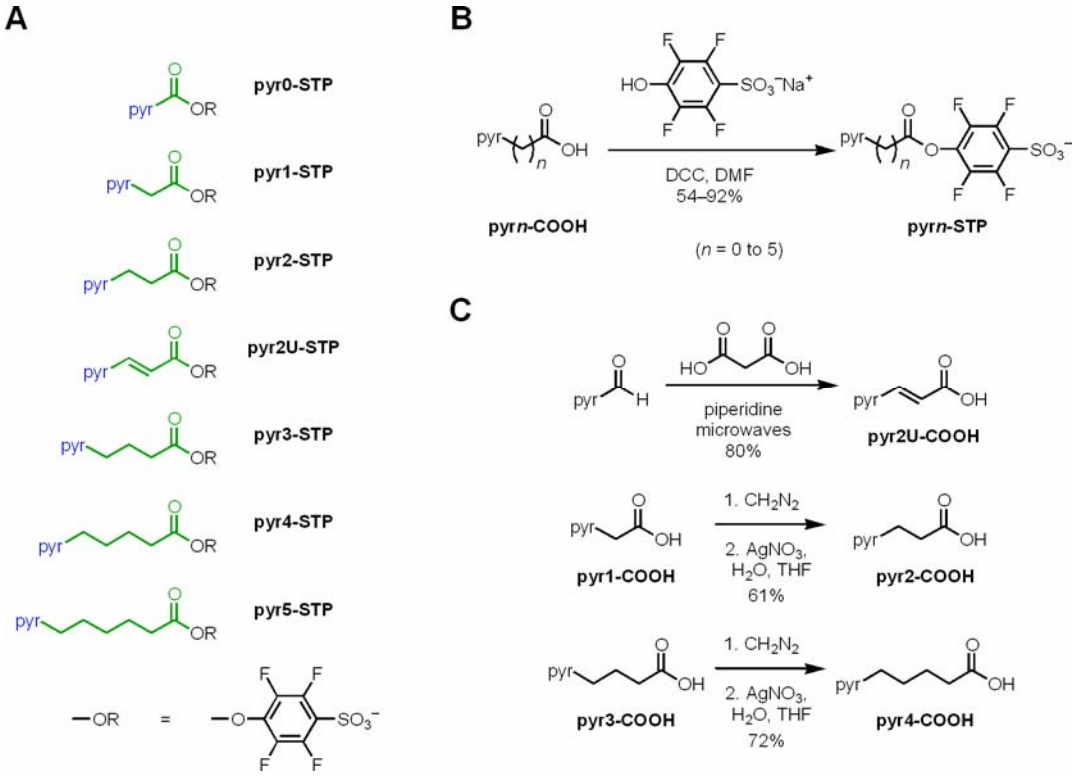

Figure X8. Pyrene STP ester structures and synthesis. (A) Pyrene esters **pyr0-STP** through **pyr5-STP**. (B) Synthesis of pyrene STP esters from pyrene carboxylic acids. (C) Synthesis of **pyr2U-COOH**, **pyr2-COOH**, and **pyr4-COOH**.

General considerations for organic synthesis procedures

Reagents used were of commercial grade and were used without purification unless otherwise indicated. Dry solvents were obtained from Acros Acroseal bottles (DMF), by passage through activated neutral alumina under positive argon pressure (THF), or by distillation from sodium (benzene). All reactions were performed under positive argon pressure. Thin-layer chromatography (TLC) was performed on silica gel plates pre-coated with fluorescence indicator with visualization by UV light (254 nm). Silica gel (230-400 mesh) was used for column chromatography. NMR spectra were obtained on Varian NMR spectrometers at the indicated frequencies. ^{1}H and ^{13}C chemical shifts in parts per million (δ) were referenced to internal tetramethylsilane (TMS). ^{19}F chemical shifts in δ were referenced to external 1% CF_3CO_2D in D_2O at –76.53 ppm, where $CFCl_3$ is at 0 ppm. Infrared (IR) spectra were obtained using a Perkin Elmer Spectrum BX spectrophotometer referenced to a polystyrene standard. Mass spectrometry data were obtained at the UIUC School of Chemical Sciences

mass spectrometry laboratory using a Micromass ZAB-SE or 70-SE-4F instrument (EI), a Micromass Q-Tof Ultima instrument (ESI), or a Voyager SE-DTR instrument (MALDI).

Synthesis procedures for pyrene STP esters

General procedure for synthesis of pyrene STP esters: **pyr3-STP.** This procedure is representative for formation of STP esters from the analogous carboxylic acid. The reagents **pyr3-COOH** (100 mg, 0.41 mmol, 1.0 equiv) and 4-sulfo-2,3,5,6-tetrafluorophenol sodium salt (NaSTP, 236 mg, 0.82 mmol, 2.0 equiv) (23) were dissolved in DMF (10 mL). Dicyclohexylcarbodiimide (DCC, 128 mg, 0.62 mmol, 1.5 equiv) was added, and the mixture was stirred for 46 h. The mixture was filtered, and the precipitated dicyclohexylurea (DCU) was washed with EtOAc (15 mL). In some cases, THF instead of EtOAc was used for the rinse. The filtrates were concentrated and the solid was chromatographed, eluting with a gradient from 0–15% MeOH in $CHCl_3$ to afford 128 mg (0.25 mmol, 61%) of **pyr3-STP** as a white solid. R_f 0.45 (1:3 MeOH:$CHCl_3$). ^{1}H NMR (500 MHz, DMSO-d_6) δ 8.45-7.95 (m, 9H), 3.44 (t, J = 7.75 Hz, 2H), 2.97 (t, J = 7.25 Hz, 2H), 2.16 (m, 2H). ^{13}C NMR (125 MHz, DMSO-d_6) δ 169.6, 135.7, 130.9, 130.5, 129.5, 128.2, 127.56, 127.50, 126.7, 126.2, 125.1, 124.9, 124.32, 124.19, 123.4, 32.3, 31.6, 26.6. ^{19}F NMR (470 MHz, DMSO-d_6) δ –139.8 (t, 2F), –154.3 (t, 2F). FAB-MS $[M–H]^–$ 515.1. ESI-HRMS $[M–H]^–$ calcd. for $C_{26}H_{15}F_4O_5S$ 515.0576, found 515.0552. STP esters should be chromatographed and either used immediately, stored at –80°C in 50 mM DMF or DMSO solution, or stored at –20 °C as a dry solid.

pyr0-STP. The reagents **pyr0-COOH** (50 mg, 0.203 mmol, 1.0 equiv), NaSTP (100 mg, 0.41 mmol, 2.0 equiv) and DCC (63 mg, 0.305 mmol, 1.5 equiv) were combined in DMF (6 mL) for 50 h and purified as in the general procedure to afford 68 mg (0.14 mmol, 71%) of **pyr0-STP** as a pale yellow solid. R_f 0.48 (1:3 MeOH:$CHCl_3$). ^{1}H NMR (500 MHz, DMSO-d_6) δ 9.12-8.18 (m, 9H). ^{13}C NMR (125 MHz, DMSO-d_6) δ 163.4, 136.0, 132.0, 131.5, 131.0, 130.1, 129.9, 128.1, 127.79, 127.71, 125.3, 124.4, 123.8, 123.4, 118.6, 109.9. ^{19}F NMR (470 MHz, DMSO-d_6) δ –139.7 (m, 2F), –154.2 (m, 2F). FAB-MS $[M–H]^–$ 473.1. ESI-HRMS $[M–H]^–$ calcd. for $C_{23}H_9F_4O_5S$ 473.0106, found 473.0089.

pyr1-STP. The reagents **pyr1-COOH** (50 mg, 0.19 mmol, 1.0 equiv), NaSTP (94 mg, 0.38 mmol, 2.0 equiv), and DCC (59 mg, 0.28 mmol, 1.5 equiv) were combined in DMF (6 mL) for 45 h and purified as in the general procedure to afford 79 mg (0.16 mmol, 80%) of **pyr1-STP** as a white solid. R_f 0.53 (1:3 MeOH:$CHCl_3$). ^{1}H NMR (500 MHz, DMSO-d_6) δ 8.4-8.0 (m, 9H), 4.98 (s, 2H). ^{13}C NMR (125 MHz, DMSO-d_6) δ 168.8, 131.3, 131.1, 130.8, 129.6, 129.4, 128.5, 127.97, 127.89, 127.7, 127.0, 126.1, 125.9, 125.5, 124.7, 124.3, 123.7, 37.7. ^{19}F NMR (470 MHz, DMSO-d_6) δ –139.8 (m, 2F), –154.3 (m, 2F). FAB-MS $[M–H]^–$ 487.1. ESI-HRMS $[M–H]^–$ calcd. for $C_{24}H_{11}F_4O_5S$ 487.0263, found 487.0256.

pyr2-COOH (24). This compound was synthesized by Arndt-Eistert homologation from **pyr1-COOH**. (*i*) Acid chloride formation. A portion of **pyr1-COOH** (0.327 g, 1.25 mmol, 1.0 equiv) was dissolved in benzene (7.5 mL). Thionyl chloride (0.30 mL, 3.9 mmol, 2.8 equiv) was added dropwise over 10 min. The dark red mixture was refluxed for 6 h and concentrated under vacuum, providing **pyr1-COCl** (0.348 g, 1.25 mmol) as a reddish-brown solid that was used without further purification. (*ii*) Diazoketone formation. Diazald (1.64 g, 7.63 mmol, 6.1 equiv) was dissolved in diethyl ether (60 mL). Potassium hydroxide (5.0 g, 89.1 mmol, 63.6 equiv) was dissolved in ethanol (10 mL) and H_2O (8 mL) and heated to 65 °C. Behind a blast shield, the Diazald solution was added dropwise to the potassium hydroxide solution via an addition funnel. The generated diazomethane was collected in a flask at –10 °C containing ether (50 mL) for 20 min, until the ether solution was yellow. The acid chloride **pyr1-COCl** (0.348 g, 1.25 mmol, 1.0 equiv) was dissolved in ether (40 mL) and added to the

flask containing diazomethane in ether over 15 min via syringe, during which time diazomethane was still being generated. After 20 min, the remaining Diazald solution was quenched with acetic acid (2 mL). The reaction flask containing excess diazomethane was carefully removed from the apparatus and nitrogen gas was blown over the surface of the solution to remove diazomethane and ether. After 1.5 h, the remaining ether was removed under vacuum, affording 0.391 g (1.37 mmol, 110% of the theoretical yield) of diazoketone **pyr1-COCHN$_2$**. The brown solid was used without purification due to its instability on silica gel. R_f 0.59 (2:1 hexane:EtOAc). ^{1}H NMR (500 MHz, $CDCl_3$) δ 8.26-7.83 (m, 9H), 4.87 (br s, 2H), 4.30 (s, 2H). ^{13}C NMR (125 MHz, $CDCl_3$) δ 193.8, 178.1, 131.5, 131.3, 130.9, 129.8, 128.71, 128.60, 127.8, 127.5, 126.4, 125.74, 125.61, 125.33, 125.25, 125.17, 123.3, 55.5, 46.7, 35.9, 28.6. IR 2103 cm^{-1} (C=N$^+$=N$^-$), 1634 cm^{-1} (C=O), 1352 cm^{-1} (C=N$^+$=N$^-$). (*iii*) Wolff rearrangement. The diazoketone **pyr1-COCHN$_2$** (0.210 g, 0.73 mmol, 1.0 equiv) was dissolved in THF (12 mL) and water (6 mL), and silver nitrate (0.129 g, 0.77 mmol, 1.05 equiv) was added. The solution was stirred at room temperature for 25 h. THF was removed under vacuum, and the residue was partitioned between EtOAc (50 mL) and water (50 mL). The aqueous layer was extracted with EtOAc (2 × 50 mL). The combined organic extracts were dried over Na_2SO_4, concentrated under vacuum, and chromatographed, eluting with 3:7 hexane:EtOAc containing 2% acetic acid to afford 0.121 g (0.44 mmol, 61%) of **pyr2-COOH** as a brown pasty solid. R_f 0.37 (2:1 hexane:EtOAc). ^{1}H NMR (500 MHz, acetone-d_6) δ 8.39-7.99 (m, 9H), 3.68 (t, J = 8.0 Hz, 2H), 2.87 (t, J = 7.75 Hz, 2H). ^{13}C NMR (125 MHz, acetone-d_6) δ 205.7, 173.4, 127.73, 127.71, 127.5, 126.9, 126.3, 125.26, 125.21, 125.13, 123.4, 110.0, 67.4, 35.5, 25.5.

pyr2-STP. The reagents **pyr2-COOH** (100 mg, 0.36 mmol, 1.0 equiv), NaSTP (179 mg, 0.73 mmol, 2.0 equiv), and DCC (113 mg, 0.55 mmol, 1.5 equiv) were combined in DMF (8 mL) for 26 h and purified as in the general procedure to afford 98 mg (0.20 mmol, 54%) of **pyr2-STP** as a white solid. R_f 0.50 (1:3 MeOH:$CHCl_3$). ^{1}H NMR (500 MHz, DMSO-d_6) δ 8.44-8.04 (m, 9H), 3.77 (t, J = 7.5 Hz, 2H), 3.33 (t, J = 7.75 Hz, 2H). ^{13}C NMR (125 MHz, DMSO-d_6) δ 169.0, 133.9, 130.9, 130.4, 129.8, 129.0, 128.2, 128.0, 127.7, 127.47, 127.31, 126.9, 126.3, 125.5, 125.21, 125.08, 125.0, 124.22, 124.09, 123.8, 123.2, 34.3, 27.4. ^{19}F NMR (376 MHz, DMSO-d_6) δ –139.7 (m, 2F), –153.9 (m, 2F). FAB-MS [M–H]$^-$ 501.1. ESI-HRMS [M–H]$^-$ calcd. for $C_{25}H_{13}F_4O_5S$ 501.0419, found 501.0416.

pyr2U-STP. The reagents **pyr2U-COOH** (75 mg, 0.24 mmol, 1.0 equiv; synthesized from 1-pyrenecarboxaldehyde and malonic acid as reported (25-28) using microwave assistance (29,30)), NaSTP (118 mg, 0.48 mmol, 2.0 equiv) and DCC (74 mg, 0.36 mmol, 1.5 equiv) were combined in DMF (6 mL) for 42 h and purified as in the general procedure to afford 92 mg (0.20 mmol, 82%) of **pyr2U-STP** as a bright yellow solid.. R_f 0.45 (1:3 MeOH:$CHCl_3$). ^{1}H NMR (500 MHz, DMSO-d_6) δ 9.12 (d, J = 16.0 Hz, 1H), 8.74-8.12 (m, 9H), 7.34 (d, J = 16.0 Hz, 1H). ^{13}C NMR (125 MHz, DMSO-d_6) δ 165.1, 162.7, 145.5, 133.2, 130.8, 130.182, 130.167, 129.9, 129.39, 129.29, 127.45, 127.42, 126.88, 126.86, 126.70, 126.61, 126.46, 126.39, 125.47, 125.45, 125.25, 124.0, 123.6, 115.9. ^{19}F NMR (470 MHz, DMSO-d_6) δ –139.9 (m, 2F), –154.3 (m, 2F). ESI-MS [M–H]$^-$ 499.0. ESI–HRMS [M–H]$^-$ calcd. for $C_{25}H_{11}F_4O_5S$ 499.0263, found 499.0255.

pyr4-COOH. This compound was synthesized by Arndt-Eistert homologation from **pyr3-COOH**. (*i*) Acid chloride formation (31-33). A portion of **pyr3-COOH** (0.500 g, 1.73 mmol, 1.0 equiv) was dissolved in benzene (10 mL). Thionyl chloride (0.38 mL, 4.9 mmol, 2.8 equiv) was added dropwise over 10 min. The mixture was refluxed for 7 h and concentrated under vacuum, providing **pyr3-COCl** (0.485 g, 1.58 mmol) as a pale yellow solid that was used without further purification. (*ii*) Diazoketone formation. Diazald (2.5 g, 11.7 mmol, 8.4 equiv) was dissolved in diethyl ether (60 mL). Potassium hydroxide (5 g, 89.1 mmol, 63.6 equiv) was dissolved in ethanol (10 mL) and H_2O (8 mL) and heated to 65 °C. Behind a blast shield, the Diazald solution was added dropwise to the potassium hydroxide

solution via an addition funnel. The generated diazomethane was collected in a flask at –10 °C containing ether (50 mL) for 20 min, until the ether solution was yellow. The acid chloride **pyr3-COCl** (0.431 g, 1.4 mmol, 1.0 equiv) was dissolved in ether (40 mL) and added to the flask containing diazomethane in ether over 15 min via syringe, during which time diazomethane was still being generated. After 20 min, the remaining Diazald solution was quenched with acetic acid (2 mL). The reaction flask containing excess diazomethane was carefully removed from the apparatus and nitrogen gas was blown over the surface of the solution to remove diazomethane and ether. After 1.5 h, the remaining ether was removed under vacuum, affording 0.459 g (1.52 mmol, 108% of the theoretical yield) of diazoketone **pyr3-COCHN$_2$**. The light brown solid was used without purification due to its instability on silica gel. R_f 0.59 (2:1 hexane:EtOAc). ^{1}H NMR (400 MHz, $CDCl_3$) δ 8.4-7.8 (m, 9H), 5.2 (br s, 1H), 3.4 (t, J = 6.0 Hz, 2H), 2.4 (br s, 2H), 2.2 (quintet, J = 6.0 Hz, 2H). ^{13}C NMR (125 MHz, $CDCl_3$) δ 195.0, 131.7, 127.73, 127.66, 127.0, 126.1, 125.32, 125.19, 125.06, 123.6, 48.5, 40.5, 39.2, 32.9. IR 2099 cm^{-1} (C=N$^+$=N$^-$), 1638 cm^{-1} (C=O), 1376 cm^{-1} (C=N$^+$=N$^-$). (*iii*) Wolff rearrangement. The diazoketone **pyr3-COCHN$_2$** (0.230 g, 0.74 mmol, 1.0 equiv) was dissolved in THF (15 mL) and water (7.5 mL), and silver nitrate (0.131 g, 0.77 mmol, 1.05 equiv) was added. The solution was stirred at room temperature for 20 h. THF was removed under vacuum, and the residue was partitioned between EtOAc (50 mL) and water (50 mL). The aqueous layer was extracted with EtOAc (2 × 50 mL). The combined organic extracts were dried over Na_2SO_4, concentrated under vacuum, and chromatographed, eluting with 3:7 hexane:EtOAc containing 2% acetic acid to afford 0.162 g (0.54 mmol, 72%) of **pyr4-COOH** as a white solid. R_f 0.37 (2:1 hexane:EtOAc). ^{1}H NMR (400 MHz, acetone-d_6) δ 8.5–7.9 (m, 9H), 3.42 (t, J = 7.8 Hz, 2H), 2.40 (t, J = 7.4 Hz, 2H), 1.92 (quintet, J = 7.4 Hz, 2H), 1.82 (quintet, J = 7.4 Hz, 2H). ^{13}C NMR (100 MHz, acetone-d_6) δ 205.5, 127.76, 127.70, 127.4, 126.8, 126.2, 125.16, 125.10, 124.97, 123.8, 122.6, 33.4, 33.1, 31.5, 25.1.

pyr4-STP. The reagents **pyr4-COOH** (70 mg, 0.23 mmol, 1.0 equiv), NaSTP (132 mg, 0.46 mmol, 2.0 equiv) and DCC (72 mg, 0.35 mmol, 1.5 equiv) were combined in DMF (6 mL) for 46 h and purified as in the general procedure to afford 112 mg (0.21 mmol, 92%) of **pyr4-STP** as a pale yellow solid. R_f 0.45 (1:3 MeOH:$CHCl_3$). ^{1}H NMR (400 MHz, DMSO-d_6) δ 8.40-7.95 (m, 9H), 3.36 (t, J = 7.25 Hz, 2H), 2.89 (t, J = 6.75 Hz, 2H), 1.87 (m, 4H). ^{13}C NMR (125 MHz, DMSO-d_6) δ 169.7, 136.6, 131.0, 130.5, 129.3, 128.1, 127.51, 127.47, 127.2, 126.6, 126.2, 125.0, 124.8, 124.29, 124.21, 123.5, 32.4, 32.2, 30.5, 24.3. ^{19}F NMR (376 MHz, DMSO-d_6) δ–139.8 (t, 2F), –154.0 (t, 2F). FAB-MS [M–H]$^-$ 529.1. ESI-HRMS [M–H]$^-$ calcd. for $C_{27}H_{17}F_4O_5S$ 529.0732, found 529.0733.

pyr5-STP. The reagents 1-pyrenehexanoic acid (30 mg, 0.095 mmol, 1.0 equiv, Molecular Probes), NaSTP (44 mg, 0.18 mmol, 2.0 equiv) and DCC (28 mg, 0.135 mmol, 1.5 equiv) were combined in DMF (5 mL) for 36 h and purified as in the general procedure to afford 40 mg (0.076 mmol, 80%) of **pyr5-STP** as a yellow solid. R_f 0.45 (1:3 MeOH:$CHCl_3$). ^{1}H NMR (500 MHz, DMSO-d_6) δ 8.36-7.94 (m, 9H), 3.34 (t, J = 7.75 Hz, 2H), 2.77 (t, J = 7.5 Hz, 2H), 1.82 (quintet, J = 7.5 Hz, 2H), 1.75 (quintet, J = 7.5 Hz, 2H), 1.53 (quintet, J = 7.63 Hz, 2H). ^{13}C NMR (125 MHz, DMSO-d_6) δ 193.8, 159.9, 159.6, 157.4, 154.8, 152.5, 150.2, 145.0, 133.5, 123.7, 111.2, 110.0, 108.2, 102.7, 96.6, 82.1, 45.3, 45.10, 45.05, 13.02, 12.95. ^{19}F NMR (470 MHz, DMSO-d_6) δ –139.8 (t, 2F), –154.5 (t, 2F). ESI-MS [M–H]$^-$ 543.2. ESI-HRMS [M–H]$^-$ calcd. for $C_{24}H_{11}F_4O_5S$ 543.0889, found 543.0899.

^{1}H and ^{19}F NMR spectra of the pyrene STP esters

The following pages show images of the ^{1}H and ^{19}F NMR spectra of **pyr0-STP** through **pyr5-STP**. In the ^{1}H NMR spectra, peaks not assigned to the indicated compound are labeled as follows: w = water; n = NMR solvent; s = common solvent (e.g., MeOH, EtOH, or EtOAc); x = unidentified impurity.